

RESEARCH ARTICLE | MAY 28 2024

Development of a direct process for the production of long glass fiber reinforced phenolic resins

Robert Maertens ✉; Wilfried Liebig; Kay André Weidenmann; Peter Elsner



AIP Conf. Proc. 3012, 020012 (2024)

<https://doi.org/10.1063/5.0194827>



AIP Advances

Why Publish With Us?

- 25 DAYS**
average time to 1st decision
- 740+ DOWNLOADS**
average per article
- INCLUSIVE**
scope

[Learn More](#)

Development of a Direct Process for the Production of Long Glass Fiber Reinforced Phenolic Resins

Robert Maertens^{1,2,a)}, Wilfried Liebig¹, Kay André Weidenmann³, Peter Elsner^{1,2,†}

¹ *Karlsruhe Institute of Technology (KIT), Institute for Applied Materials – Material Science and Engineering (IAM-WK), 76131 Karlsruhe, Germany*

² *Fraunhofer Institute for Chemical Technology ICT, 76327 Pfinztal, Germany*

³ *Augsburg University, Institute of Materials Resource Management (MRM), 86159 Augsburg, Germany*

a) *Corresponding author: robert.maertens@ict.fraunhofer.de*

Abstract. Parts made from phenolic molding compounds reinforced with glass fibers have a good heat resistance, a high dimensional accuracy, and an excellent chemical resistance. However, these parts typically have a low elongation at break and a low impact toughness. Conventional glass fiber-reinforced phenolic molding compounds have an average fiber length which is below the critical fiber length for this material combination. To increase the fiber length in the molded parts, a new injection molding process was developed, which allows the direct feeding of long glass fibers into the plasticizing unit of the injection molding machine. For opening and dispersing long fiber bundles, a thermoset-specific screw mixing element was developed and compared to the conventional conveying screw geometry. The process stability was quantified by analyzing the plasticizing work and injection work. Despite the increased fiber shortening when using the mixing element, the dynamical mechanical properties were improved compared to the standard conveying screw geometry, which is attributed to the better fiber-matrix homogenization.

INTRODUCTION

Fiber-reinforced phenolic molding compounds

Since their invention by Baekeland in 1909 [1], phenolic resins have been used in a wide variety of applications and serve as important constituents in wood composite adhesives, foams and insulation material, refractories as well as in fiber-reinforced molding compounds [2]. These composite parts have a high maximum operating temperature, an excellent chemical resistance, and a very good dimensional accuracy, which is why they are often used in the direct vicinity of the internal combustion engine [3] or electric motors [4]. One of the biggest challenges for the wider use of phenolic molding compounds is their brittle deformation behavior [5,6]. To increase the mechanical strength, reinforcement fibers are compounded into the resin. In general high average fiber lengths are desirable [7–9]. However, in the state-of-the-art thermoset injection molding process of phenolic molding compounds, small weighted average fiber length values of $L_p = 0.3 \text{ mm} \dots 0.35 \text{ mm}$ are typical [10]. To quantify the required fiber length for a significant improvement of the mechanical properties, the critical fiber length L_c , which is the minimum fiber length that is required for fully utilizing the reinforcement potential of the fibers [11], is used. A fiber length $L < L_c$ still leads to a reinforcing effect, but does not fully utilize the available potential. The literature values for L_c in glass fiber-reinforced phenolic resins vary between $L_c = 2 \text{ mm}$ [12] and $L_c = 8 \text{ mm}$ [13], so it can be assumed that the fiber length in typical, commercially available materials is significantly below L_c .

Long fiber injection molding processes

A logical first step for increasing the fiber length in the molded component is to increase the fiber length in the granulate. For thermoplastic polymers, a variety of long fiber granulates are commercially available. For thermoset matrix systems, no long fiber granulate for injection molding is available, but there are a few long fiber phenolic molding compounds for compression processing. They have a plate-like shape and are available in length classes of 5 mm, 12 mm and 24 mm. For compression molding applications, impact strength values that are 10 ... 20 times superior to conventional short fiber molding compounds are claimed [5]. However, the claimed datasheet values are in stark contrast to experimental results: According to studies by Saalbach et al. [14] and Raschke [15], these materials cause significant processing problems during injection molding, such as sticking to the screw and the barrel, without offering any beneficial mechanical properties compared to traditional short fiber molding compounds.

Several injection molding process variants with a direct long fiber feeding were developed for thermoplastic materials. In the injection molding compounder (IMC), a co-rotating twin-screw extruder is combined with a melt buffer and an injection unit [16]. To make the direct compounding cost-feasible for lower volume applications, several processes with the common aspect that the melting and compounding is carried out discontinuously have been developed. This removes the need for a melt buffer and therefore reduces the machine complexity and price. The direct compounding injection molding (DCIM) process couples a single screw compounding extruder with a traditional injection molding machine [17]. In the DIF process (direct incorporation of continuous fibers), continuous fibers are directly pulled into the screw of the injection molding machine [18]. Mixing elements on the injection molding screw are required to achieve a good fiber dispersion. The fiber direct compounding process (FDC) works by pulling the unreinforced granulate out of the hopper into the screw, where it is melted like in a conventional injection molding machine [19]. In contrast the DIF process, the continuous fibers are cut to a length of $L = 2 \text{ mm} \dots 100 \text{ mm}$ with a fiber chopper and are fed to the injection molding machine via a twin-screw sidefeed. At the position of the fiber feed, the screw core diameter is reduced to facilitate the incorporation of the fibers. In this publication, the development of a long fiber thermoset molding process is described. The fiber length in the molded components and their mechanical properties are evaluated.

Data acquisition during the injection molding process

The quantification of energy input into the polymer during plasticization and injection is particularly important for reactive thermoset materials, such as phenolic resins. The screw torque during the plasticizing process M_{Plast} was monitored and analyzed by several authors. According to Rauwendaal [20], it is a good measure to quantify the mechanical power consumed by the extrusion process. For hydraulic injection molding machines, this plasticizing torque is typically calculated by measuring the pressure drop Δp_{Hydr} over the screw drive according to Equation (1)

$$M_{\text{Plast}} = \frac{\Delta p_{\text{Hydr}} \eta_{\text{Hydr}} V_{\text{Drive}}}{20\pi}, \quad (1)$$

using the hydraulic efficiency η_{Hydr} and the hydraulic volume of the drive V_{Drive} . Several authors [21,22] used the injection work W_{Plast} , which is the integral of the plasticizing power P_{Plast} , as a measure for the total energy input into the polymer during the plasticization phase, see Equation (2).

$$\begin{aligned} W_{\text{Plast}} &= \int_{\text{PlSt}}^{\text{PlEnd}} P_{\text{Plast}} dt = \int_{\text{PlSt}}^{\text{PlEnd}} (M_{\text{Plast}} \times \omega) dt \\ &= 2\pi \int_{\text{PlSt}}^{\text{PlEnd}} (M_{\text{Plast}} \times n) dt \end{aligned} \quad (2)$$

In Equation (2), M_{Plast} is the plasticizing torque and n is the screw rotational speed. For a standard injection molding process using thermoplastic materials, Kruppa [21] observed an increase of the plasticizing work with increasing screw speed. This increased energy input leads to a stronger shortening of glass fibers, as described by Truckenmüller [23]. With increasing plasticizing work, fiber length asymptotically approaches a threshold value, which is independent of initial fiber length and glass fiber content. A similar approach to quantify the energy input into the material during the injection phase of the process is the calculation of the injection work W_{Inj} , which is the integral of the injection force F_{Inj} over the injection stroke distance s according to Equation (3).

$$W_{\text{Inj}} = \int_{\text{Inj}_{\text{st}}}^{\text{Inj}_{\text{End}}} F_{\text{Inj}} \, ds = A_{\text{Piston}} \int_{\text{Inj}_{\text{st}}}^{\text{Inj}_{\text{End}}} p_{\text{Hydr.,Inj}} \, ds \quad (3)$$

Lucyshyn et al. [24] as well as Schiffers [25] use the injection work as a measure for viscosity changes of thermoplastic polymers during the process, e.g. due to a change in moisture content. Cavic [26] used the injection work for judging the reproducibility of the injection molding process. All cited works deal with thermoplastic materials. The usage of the injection work to evaluate the curing state of the material in the thermoset injection molding processes has not been reported yet. In this work, the injection work is used in conjunction with the plasticizing work for describing the process stability of the thermoset injection molding process.

MATERIALS AND METHODS

Materials and manufacturing processes

The phenolic molding compound used for the process development is based on the Vyncolit® X6952 short glass fiber-reinforced compound by Sumitomo Bakelite (Gent, Belgium). The short glass fibers (SGF) DS5163-13P $D = 13 \mu\text{m}$ were sourced from 3B fibreglass (Hoeilaart, Belgium) as chopped strands. The SGF content in the molding compound was adjusted from fractions of $\phi = 0 \text{ wt.-%}$ up to $\phi = 60 \text{ wt.-%}$ by twin-screw extruder compounding on a lab scale extruder with a screw diameter of $d = 27 \text{ mm}$ (Leistritz Extrusionstechnik GmbH, Nürnberg, Germany) [27]. For the long glass fibers (LGF), the $Tt = 2400 \text{ tex}$ direct roving 111AX11 with a filament diameter of $D = 17 \mu\text{m}$ by 3B fibreglass was used. The nomenclature of the material formulations follows the scheme PF-SGF x -LGF y . The variables x and y stand for the fiber content ϕ of the short or long glass fibers. The long fiber thermoset injection molding process enables a flexible combination of SGF and LGF by separating the two mass flows, see Figure 1.

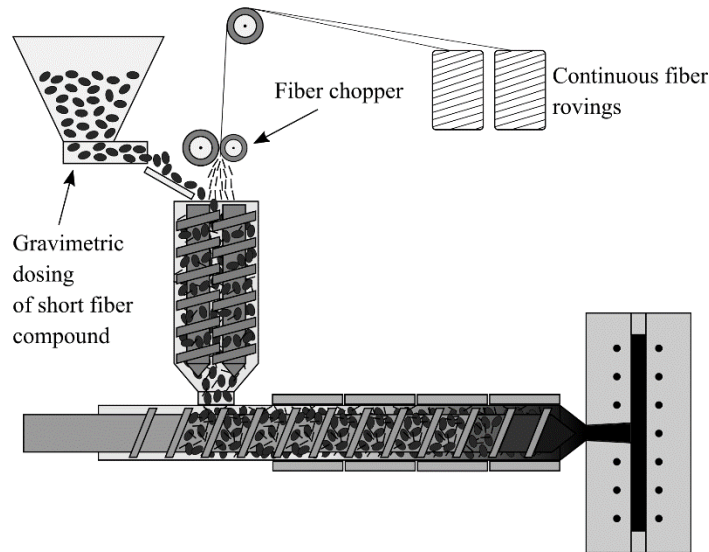


Figure 1. Process scheme long fiber thermoset injection molding process

The SGF are gravimetrically fed as a part of the phenolic molding compound, whereas the LGF are chopped from the continuous rovings. Both are fed into the plasticizing unit with a twin-screw sidefeed. The injection molding screw is a conveying screw with an interchangeable screw tip, which allows the adaption of either a conventional conveying geometry or a newly designed, thermoset specific Maddock mixing element, which is shown in Figure 2a).

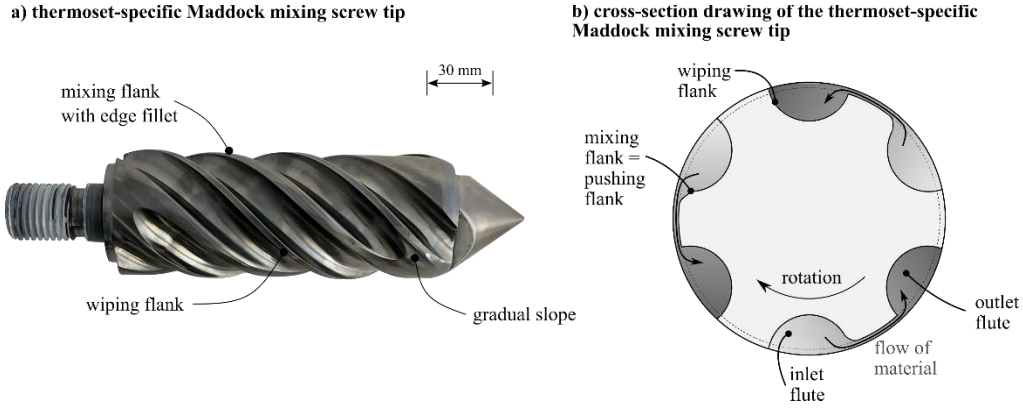


Figure 2. Thermoset-specific Maddock mixing element image (a) and cross-section drawing (b)

The mixing element features three distinct differences to a conventional Maddock mixing element. First, the inlet channels have a gradual slope at their ends to facilitate the flow of material and to avoid material accumulations, which additionally narrows down the residence time distribution. The second feature difference is the edge fillet on the mixing flight. Due to the radius on this edge, the material undergoes additional elongational stresses when passing through the shear gap. The third main feature is that the positions of the mixing flight and wiping flight are reversed compared to the state-of-the-art, which is visible from Figure 2b). Traditionally, the pushing flank is also the wiping flank of the mixing element. This makes sense for thermoplastic materials which enter the mixing element in a completely molten state. However, due to the low shear conveying screw design, the thermoset molding compounds only start to melt in the foremost screw flights under the influence of the pressure from the flanks of the conveying screw. This means that the material close to the pushing screw flanks is molten, whereas the material distant from the screw flanks might still be granular [28]. If the molding compound entered a traditional mixing element in such a state, the granular fraction would be pushed through the shear gap, blocking it. The thermoset-specific design ensures that only molten material is pushed through the shear gap.

Material characterization techniques

In the injection molding trials, rectangular plates with a size of 190 mm × 480 mm and a thickness of $h = 4$ mm were molded. The plates were filled via a central sprue with a diameter of $d = 15$ mm and post-cured up to $T = 180$ °C. The test specimens were cut out of the plates by waterjet-cutting both in parallel (0°) and perpendicular (90°) orientation to the flow of material. The mechanical characterization was carried out according to the standards DIN EN ISO 527-2 [29] for the tensile test and DIN EN ISO 6603-2 [30] for the puncture impact test. X-ray computed tomography images were obtained by using a XYLON precision μ CT. The homogeneity of the molded parts was judged both visually and with the image texture analysis method described by Maertens et al. in [31].

For the fiber length measurement according to the method described in [10], a sample was cut from the molded part. It had a diameter of $d = 25$ mm and a typical weight of $m = 3$ g. The matrix was removed pyrolytically at $T = 650$ °C for $t = 36$ h under air atmosphere by using a LECO TGA 701 (St. Joseph, USA). Subsequently, the ash residue was transferred into distilled water and a small amount of acetic acid was added. Further dilution steps were done by using a beaker with an outlet tap and a propeller stirrer. The measurement samples were taken through the outlet tap and transferred to several petri-dishes, which were then analyzed by using the FASEP device by IDM systems (Darmstadt, Germany). Per material and process parameter combination, approximately $n = 25.000 \dots 40.000$ fibers were measured. The weighted average fiber length L_p can be calculated according to Equation (4) using the length L_i of each individual fiber i .

$$L_p = \frac{\sum_{i=1}^n n_i L_i^2}{\sum_{i=1}^n n_i} \quad (4)$$

RESULTS

Process Data Evaluation

Figure 3 shows the plasticizing work and the injection work for a process stability study using screw speeds of $n = 40$ 1/min and $n = 70$ 1/min. For both parameter combinations, 10 (trial number 1) respectively 9 (trial number 2) injection molding cycles were performed after a stable process was established.

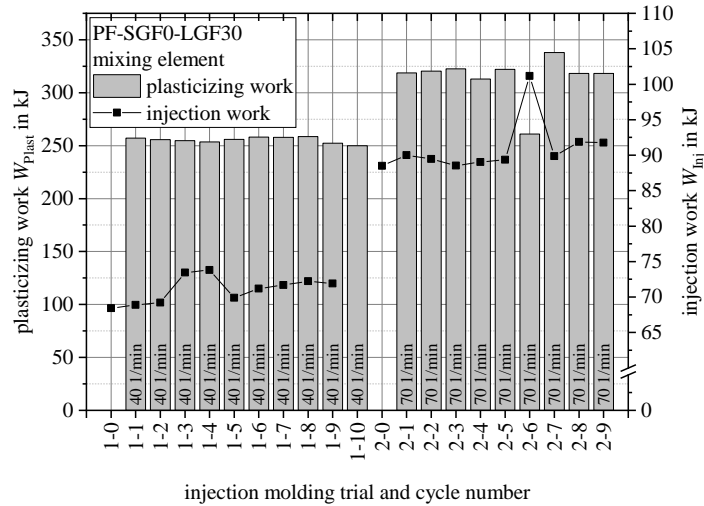


Figure 3: Plasticizing work and injection work for PF SGF0 LGF30 process stability study

For both screw speeds, the plasticizing work is stable. The effect of the increased screw speed on the plasticizing work and the injection work is visible. In contrast to the stable process shown above, Figure 4 shows an example of an unstable process. Despite the constant level of plasticizing work, the injection work rises for each injection molding cycle until no injection is possible due to cured material in the machine nozzle.

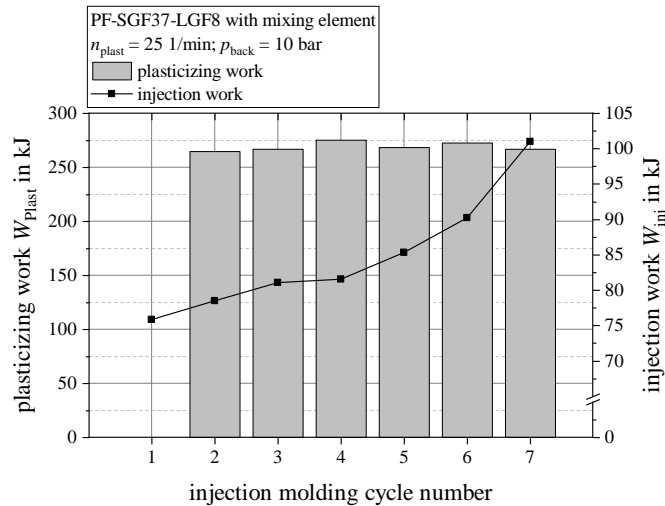


Figure 4: Plasticizing work and injection work for PF SGF37 LGF8 process stability study

Material Characterization

The fiber length measurement results for PF-SGF0-LGF30 are shown in Figure 5. A stronger fiber shortening is visible with increasing mixing energy input, this means when using the mixing element and when increasing the screw speed.

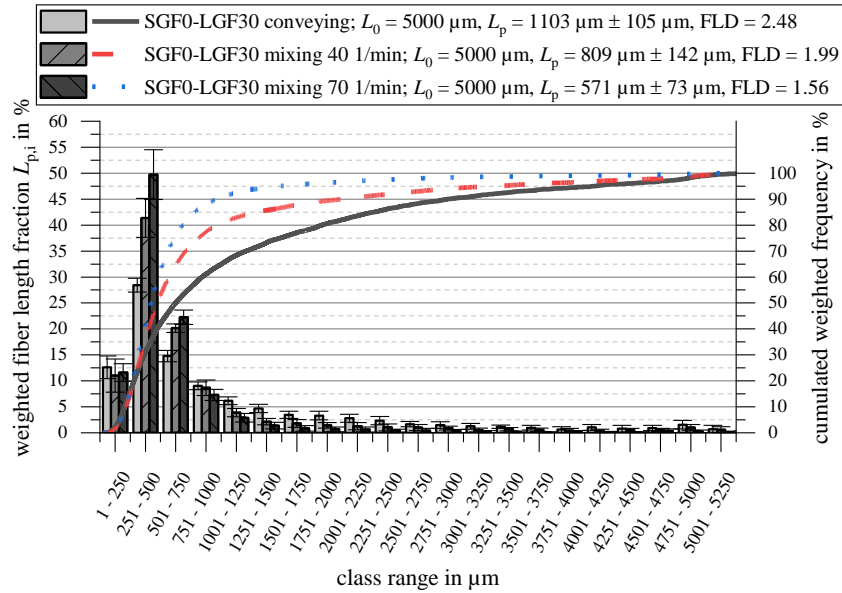


Figure 5. Weighted average fiber length for PF SGF0 LGF30 using mixing element

The weighted average fiber length in the molded part is reduced from $L_p = 1103 \mu\text{m}$ for the conveying screw tip to $L_{p, 40 \text{ 1/min}} = 809 \mu\text{m}$ and to $L_{p, 70 \text{ 1/min}} = 571 \mu\text{m}$ for the Maddock mixing element. The ratio of the weighted average fiber length and the numerical average fiber length, $\text{FLD} = L_p/L_n$, which is an indirect measure for the fiber dispersion quality [32], is also improved when using the mixing element. At the highest screw speed setting that was investigated, $\text{FLD}_{\text{mix}, 70 \text{ 1/min}} = 1.56$ indicates a good fiber dispersion. The improved homogeneity of the parts molded with the mixing element can also be seen from representative cross-sectional images, which were obtained by using X-ray computed tomography and which are shown in Figure 6.

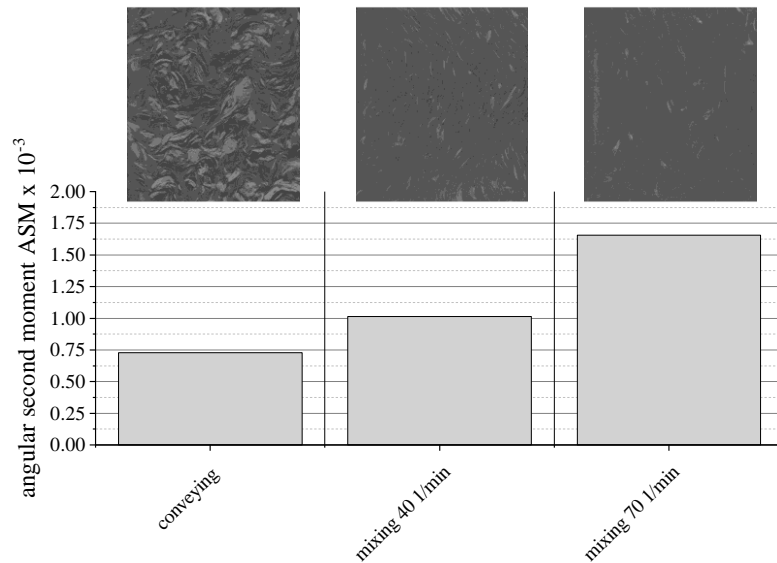


Figure 6: Angular second moment and cross-sectional images for parts molded with and without mixing element

Figure 7 shows the characterization results for the tensile strength measured according to DIN EN ISO 527 [29] parallel to the flow of material for samples with an overall total fiber content of $\phi = 30$ wt.-%.

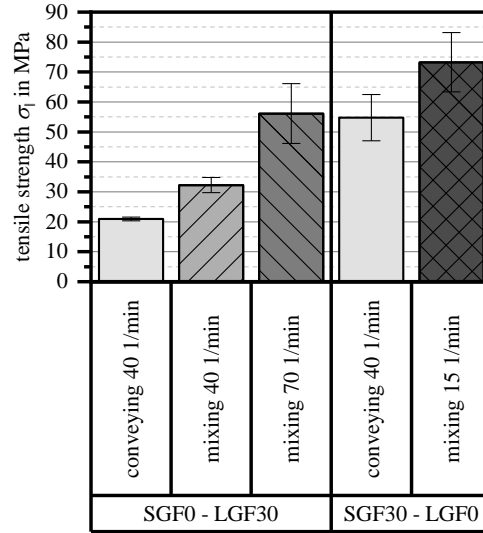


Figure 7. Tensile strength of test specimens with 30 wt.-% glass fiber content

Switching from the conveying screw geometry to the Maddock mixing screw element increases the tensile strength for all formulations and for both specimen orientations. Increasing the plasticizing screw speed when using the mixing element leads to a further significant increase in tensile strength for the PF-SGF0-LGF30 formulation in 0° orientation. For the other formulations and orientations, the tensile strength mostly increases but within the standard deviation of the measurement. The scattering of the measurement results also increases when using the mixing element. While the positive effect of the mixing element on the tensile strength of the LGF materials is clearly visible from the measurement results, it must be noted that the overall highest absolute strength value is reached by the SGF compound.

Subsequently, the dynamical mechanical properties are analyzed. Figure 8, shows the puncture impact energy measured by falling dart test according to DIN EN ISO 6603-2 [30]

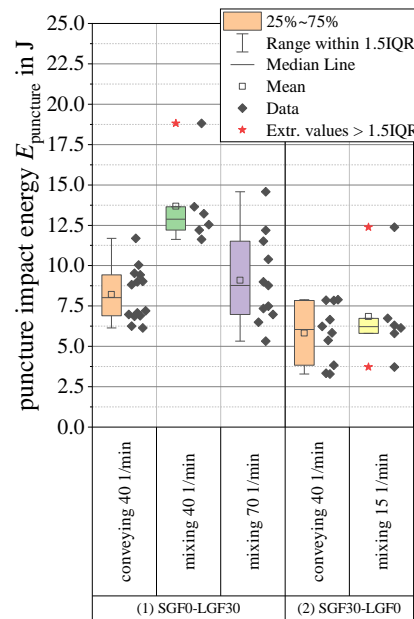


Figure 8: Puncture impact energy of 30 wt.-% specimens

For the PF-SGF0-LGF30 material, the puncture impact energy increases significantly when using the mixing element. An increase in screw speed with the mixing element has no significant effect: The average value of puncture impact energy decreases, but within the scattering of the measurement. Compared to the SGF material, the LGF formulation processed with the mixing element has a significantly higher puncture impact energy.

DISCUSSION

Switching from the conveying screw to the mixing element leads to a stronger shortening of the fibers. They are further shortened by using a higher plasticizing screw speed. This behavior is identical to the literature findings for thermoplastics. Most studies for thermoplastics found that the fiber length in the molded part decreases with higher screw rotational speed. This was confirmed for glass fiber-reinforced polypropylene (PP-GF) by Moritzer and Bürenhaus [33]. Lafranche et al. drew the same conclusions for glass fiber-reinforced polyamide 6.6 (PA66-GF) [34]. In contrast to the general consensus, Rohde et al. [35] found only a slight, but statistically insignificant shortening effect of the screw speed for PP-GF.

The mechanical characterization results shown above prove that using the mixing element leads to an increase in strength and impact toughness, despite the accompanying fiber shortening. This means that the advantage of additional mixing outweighs the disadvantage of shorter reinforcement fibers, which stands in contrast to most studies for fiber-reinforced thermoplastics. The findings of Thomason et al. [7] confirm the Kelly-Tyson model of the critical fiber length. They found that the tensile strength increases up to a fiber length of $L = 3 \text{ mm} \dots 6 \text{ mm}$ for PP-GF, which is in the range of the critical fiber length for this material. Similar results were reported by Fu and Lauke [8], who observed a rapid increase in tensile strength with increasing fiber length. However, the fiber length is only one factor that determines the strength of the composite material. Especially for thermoset composites with their brittle matrix material, the stress concentrations at inhomogeneities cannot be relieved by plastic deformation. An increased homogeneity leads to less stress concentrations and consequently to the improvement in mechanical performance, despite the fiber shortening.

The results of the puncture impact testing clearly show that the absorbed impact energy increases with increasing LGF content and is further improved by using the mixing element. The puncture impact specimens have a diameter of $d = 60 \text{ mm}$, which means that a large area is mechanically stressed during the testing. The LGF are better capable of distributing the load into this bigger area than the SGF.

SUMMARY AND CONCLUSIONS

A newly developed injection molding process variant enabled the manufacturing of parts with varying compositions of short and long glass fibers. With a purpose-designed, thermoset-specific injection molding screw mixing element, varying degrees of dispersive mixing were introduced. To obtain a stable injection molding process, the plasticizing work input into the resin had to be monitored and controlled. The molded parts were characterized regarding their tensile strength and the residual fiber length. The long fiber thermoset injection molding process enabled an up to fourfold increase of the fiber length in the parts compared to conventional phenolic molding compounds when using the standard conveying screw geometry and an approximately two times increase when using the mixing element screw. The mechanical properties of the parts increased with increased mixing energy input and thus with decreasing fiber length. It is concluded that for achieving high mechanical properties, the homogenization of the glass fibers in the phenolic resin matrix is more important than the fiber length. The addition of LGF proved to be especially beneficial for the impact toughness, which was improved by a factor of two compared to the SGF materials.

ACKNOWLEDGEMENTS

This work is funded by the Deutsche Forschungsgemeinschaft (DFG, German Research Foundation) projects EL 473/9-1 and WE 4273/18-1.

†The authors dedicate this work to the memory of our friend and colleague Prof. Dr.-Ing. Peter Elsner.

REFERENCES

1. L. H. Baekeland, Condensation product of phenol and formaldehyde and method of making the same, US942700A .
2. L. Pilato, *React. Funct. Polym.* **73**, 270 (2013).
3. T. Beran, J. Hübel, R. Maertens, S. Reuter, J. Gärtner, J. Köhler, and T. Koch, *Int. J. Refrig.* **126**, 35 (2021).
4. A. Langheck, S. Reuter, O. Saburow, R. Maertens, F. Wittemann, L. F. Berg, and M. Doppelbauer, "Evaluation of an integral injection molded housing for high power density synchronous machines with concentrated single-tooth winding," in *2018 8th International Electric Drives Production Conference*, edited by Institute of Electrical and Electronics Engineers (IEEE) (2018), p. 187.
5. K. Koizumi, T. Charles, and H. D. Keyser in *Phenolic Resins: A Century of Progress*, edited by L. A. Pilato (Springer, Berlin, Heidelberg, 2010), p. 383.
6. B.-R. Paulke, F. Börner, M. Hahn, M. Jobmann, S. Englich, M. Gehde, and H. Michael, *CIT* **87**, 1342 (2015).
7. J. L. Thomason, M. A. Vlug, G. Schipper, and H. Krikor, *Compos. Part A Appl. Sci. Manuf.* **27**, 1075 (1996).
8. S.-Y. Fu and B. Lauke, *Compos. Sci. Technol.* **56**, 1179 (1996).
9. F. Asoodeh, M. Aghvami-Panah, S. Salimian, M. Naeimirad, H. khoshnevis, and A. Zadhoush, *J. Ind. Text.* **0**, 1-20 (2021).
10. R. Maertens, A. Hees, L. Schöttl, W. V. Liebig, P. Elsner, and K. A. Weidenmann, *Polym.-Plast. Tech. Mat.* **60**, 872 (2021).
11. A. Kelly and W. R. Tyson, *J. Mech. Phys. Solids* **13**, 329 (1965).
12. F. Chen, D. Tripathi, and F. R. Jones, *Compos. Sci. Technol.* **56**, 609 (1996).
13. C. R. Gore and G. Cuff, "Long-short fiber reinforced thermoplastics," in *ANTEC 1986*, edited by Society of Plastics Engineers (Boston, 1986), p. 47.
14. H. Saalbach, T. Maenz, S. Englich, K. Raschke, T. Scheffler, S. Wolf, M. Gehde, and G. Hülder, *Faserverstärkte Duroplaste für die Großserienfertigung im Spritzgießen, Ergebnisbericht des BMBF-Verbundprojektes FiberSet* (2015).
15. K. Raschke, *Grundlagenuntersuchungen zur Prozess- und Struktursimulation von Phenolharzformmassen mit Kurz- und Langglasfaserverstärkung*, Dissertation, Technische Universität Chemnitz, 2017.
16. P. Putsch, *Compounding-injection moulding process and device*, WO92/00838 .
17. P. Hirsch, M. Menzel, J. Klehm, and P. Putsch, *Macromol. Symp.* **384**, 1 (2019).
18. F. Truckenmüller, *J. Reinf. Plast. Comp.* **12**, 624 (1993).
19. M. Holmes, *Reinf. Plast.* **62**, 154 (2018).
20. C. Rauwendaal, *Polymer extrusion*, 5th ed. (Hanser, Munich, 2014).
21. S. Kruppa, *Adaptive Prozessführung und alternative Einspritzkonzepte beim Spritzgießen von Thermoplasten*, Dissertation, Universität Duisburg-Essen, 2015.
22. G. B. M. Fischbach, *Prozessführung beim Spritzgießen härtdarer Formmassen*, Dissertation, RWTH Aachen, 1988.
23. F. Truckenmüller, *Direktverarbeitung von Endlosfasern auf Spritzgießmaschinen. Möglichkeiten und Grenzen*, Dissertation, Universität Stuttgart, 1996.
24. T. Lucyshyn, M. Kipperer, C. Kukla, G. R. Langecker, and C. Holzer, *J. Appl. Polym. Sci.* **124**, 4927-4394 (2012).
25. R. Schiffers, *Verbesserung der Prozessfähigkeit beim Spritzgießen durch Nutzung von Prozessdaten und eine neuartige Schneckenhubführung*, Dissertation, Universität Duisburg-Essen, 2009.
26. M. Cavic, *Kontinuierliche Prozessüberwachung beim Spritzgießen unter Einbeziehung von Konzepten zur Verbesserung der Schmelzequalität*, Dissertation, Universität Stuttgart, 2005.
27. R. Maertens, W. V. Liebig, P. Elsner, and K. A. Weidenmann, *J. Compos. Sci.* **127**, 1 (2021).
28. R. Singh, F. Chen, and F. R. Jones, *Polym. Compos.* **19**, 37 (1998).
29. DIN EN ISO, *527 Plastics – Determination of tensile properties* (2012).
30. DIN EN ISO, *6603-2 Plastics: Determination of puncture impact behaviour of rigid plastics. Part 2: Instrumented puncture test* (Beuth, Berlin, 2002).
31. R. Maertens, L. Schöttl, W. V. Liebig, P. Elsner, and K. A. Weidenmann, *Adv. Manuf.: Polym. Compos.* **8**, 22 (2022).
32. B. Franzén, C. Klason, T. Kubát, and T. Kitano, *Compos.* **20**, 65 (1989).

33. E. Moritzer and F. Bürenhaus, "Influence of processing parameters on fiber length degradation during injection molding," in *ANTEC 2021*, edited by Society of Plastics Engineers (Online, 2021), p. 219.
34. E. Lafranche, P. Krawczak, J.-P. Ciolczyk, and J. Maugey, *Adv. Polym. Tech.* **24**, 114 (2005).
35. M. Rohde, A. Ebel, F. Wolff-Fabris, and V. Altstädt, *IPP* **26**, 292 (2011).